Functional Materials 14, No.4 (2007)

Thermal factor effect on phase formation, structure, substructure features, and stress state in ion-plasma nano-crystalline condensates of quasi-binary WC–TiC carbide

O.V.Sobol'

National Technical University "Kharkiv Polytechnic of Institute",
21 Frunze St., 61002 Kharkiv, Ukraine

Received June 25, 2007

Using high-angle X-ray diffraction and X-ray fluorescence spectral analysis, the effects of the sputtered material composition and deposition temperature on the phase and elemental composition, structure, substructure features, and stress state in the ion-plasma quasi-binary WC–TiC coatings. The increase in relative titanium atomic content has been established to result in increasing thermal stability of the single-phase state of the ((W,Ti)C solid solution) condensate up to the temperatures exceeding 950°C at the atomic ratio Ti/W≥0.35. At atomic ratios Ti/W≤0.25 and deposition temperatures exceeding 800°C, a multi-phase condensate is formed containing the lower carbide W_2C, the essentially pure α–W phase with the BCC lattice, along with WC and TiC phases formed through (W,Ti)C solid solution decomposition. In the range of the single-phase solid solution formation, the crystallite sizes rise and the micro-strain extent drops as the condensation temperature rises. The transition into the temperature range of the multi-phase coating is followed by the micro-strain increase and the average crystallite size diminution. The carbon content in the (W,Ti)C solid solution has been estimated and the critical deposition temperature established to be 700°C; at higher temperatures, intensive vacancy formation occurs in carbon sublattice of the carbide. Physical reasons for the effects observed and the regularities revealed have been discussed.

Методами широкоугловой рентгеновской дифрактометрии и рентген-флуоресцентного спектрального анализа изучено влияние состава распыляемого материала и температуры осаждения на фазовый и элементный составы, структуру, субструктурные характеристики и напряженное состояние ионно-плазменных конденсатов квазибинарной системы WC–TiC. Установлено, что повышение относительного содержание атомов титана в конденсате приводит к увеличению верхней границы температурной стабильности однофазного ((W,Ti)C-твердый раствор) состояния осаждаемого материала, которое при соотношении атомов Ti/W≥0.35 может превышать 950°C. При соотношении атомов Ti/W≤0,25 и температуре осаждения выше 800°C происходит формирование многофазного конденсата, содержащего низший карбид W_2C, практически чистый α–W с ОЦК решеткой и WC и TiC фазы, образующиеся в результате распада (W,Ti)C-твердого раствора. Размер кристаллитов в области формирования однофазного твердого раствора с повышением температуры конденсации увеличивается, а величина микродеформации падает. Переход в температурную область формирования многофазного покрытия сопровождается увеличением микродеформации в кристаллитах и уменьшением их среднего размера. Проведена оценка содержания углерода в (W,Ti)C-твердом растворе, и установлена критическая температура осаждения 700°C, выше которой происходит интенсивное образование вакансий в углеродной подрешетке карбида.

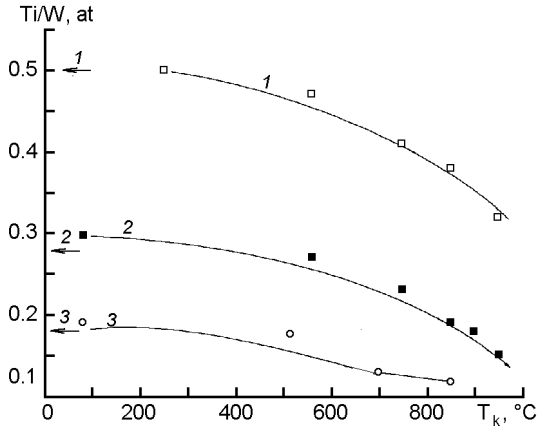

Fig. 1. Elemental composition vs deposition temperature for condensates deposited by ion-plasma sputtering of three targets differing in compositions: *1* – 31 mol.%TiC, 69 mol.% WC; *2* – 21 mol.% TiC, 79 mol.%WC; *3* – 15 mol.%, TiC, 85 mol.%WC (concentrations Ti/W in targets are given left).

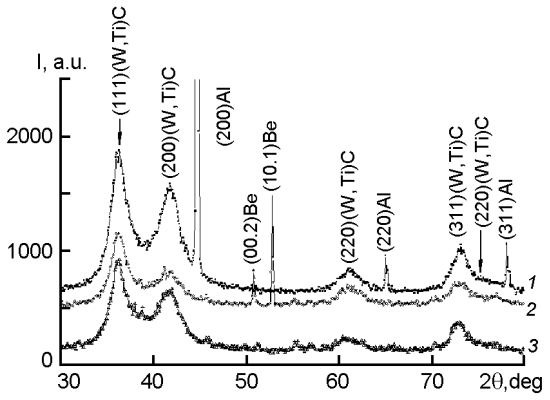

Fig. 2. Partial views of diffraction spectra for the samples 15 mol.% TiC–85 mol.% WC deposited at the condensation temperature 80°C onto different substrate types: aluminum foil (*1*), beryllium (*2*), finished single-crystalline silicon (*3*).

A feature of ion-plasma sputtered solid solution condensates is the high sensitivity of phase composition, structure, and functional properties to relatively small temperature variations under deposition thereof [1–3]. A particularly wide variety of phase compositions and structure states should be expected under condensation of the solid solutions based on quasi-binary transitional metal borides, carbides, or nitrides differing in electronic structure. The titanium-tungsten pair belongs to such transitional metals, which provides the most difference in chemical activity to non-metal atoms (titanium belongs to the IV Group, 4th period, while tungsten, to the VI Group, 6th period). In addition, a considerable difference between Ti and W in atomic masses and thus in scattering abilities makes it possible to reveal successfully the various structure changes using X-ray diffraction methods [4].

The relatively simple structure based on FCC lattice and high performance characteristics of the initial constituents make the quasi-binary WC–TiC system to be very promising for industrial applications. In addition, the simple lattice of both the constituents and the solid solution in condensed state [5] allows effective X-ray diffraction characterization of the processes therein. The purpose of this work is to establish the formation regularities of phase composition, structure, and stress state, as well as the kinetics of changes thereof at different deposition temperatures of ion-plasma nano-crystalline condensates from the example of the quasi-binary WC–TiC system with a cubic lattice.

The samples were prepared by ion sputtering of the hot-pressed targets with different WC and TiC contents: the 1st target contained 31 mol.% TiC and 69 mol.% WC; the 2nd, 21 mol.% TiC and 79 mol.% WC; the 3rd, 15 mol.% TiC and 85 mol.% WC. The planar magnetron scheme was applied. The ion sputtering was carried out in the Ar atmosphere under 0.2 to 0.4 Pa pressure. The sputtering voltage was 320 to 400 V, thus providing the condensation rate about 0.5 nm/s. As substrates, 15 μm thick aluminum and beryllium rolled foils, polished nickel, and polished both single-crystal silicon and finished glass ceramic of 380 and 350 μm thickness, respectively, were used. The phase composition, structure, substructure features (coherence length and microstrain), and stress state were studied by the standard X-ray diffraction method using a DRON-3 instrument with Cu–K_α radiation [1, 3]. The more detailed X-ray diffraction patterns were measured on the samples deposited onto silicon and beryllium substrates, while others (on aluminum, nickel, and glass ceramic substrates) were used for some comparative investigations.

Elemental compositions were studied by X-ray fluorescence spectrometry using a SPRUT instrument (produced by AS "Ukrrentgen", Ukraine). The exciting radiation was provided by an X-ray tube with silver anode.

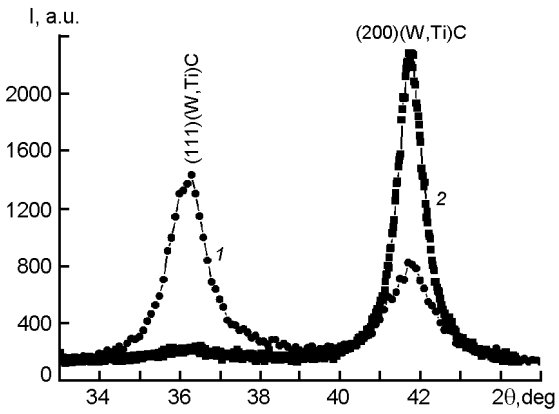

Fig. 3. Partial views of diffraction spectra for the condensate deposited at 300°C temperature by sputtering of the 2nd target onto beryllium (*1*) and silicon (*2*) substrates.

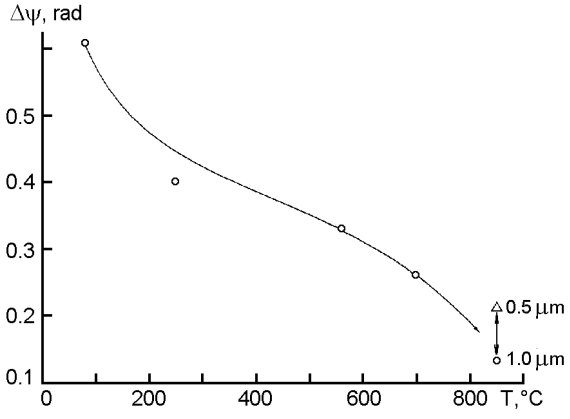

Fig. 4. Variation of the [100] texture perfection degree in the 1 μm thick condensates deposited onto silicon substrate by sputtering the 3rd target.

The elemental analysis by X-ray fluorescence spectrometry has shown the Ti/W metal atomic ratio to be almost constant and close to the target composition for the coatings deposited at temperatures ≤500°C (Fig. 1). At higher condensation temperatures, the atomic ratio of lighter Ti to heavier W decreases.

For the condensates obtained both at nearly ambient temperature and elevated ones (up to 750°C), the formation of the single-phase (W,Ti)C solid solution [6] with nano-crystalline structure [7] was observed in a wide composition range. Note that at lower condensation temperatures (80–250°C), practically the same structure state is realized on all the types of the substrates used (Fig. 2). At higher deposition temperatures, beginning from 300°C, oriented crystallites (with [100] axis normal to the growth plane) were formed predominantly on the smooth polished nickel substrates and finished glass ceramic ones. No predominant crystallite orientation was observed in the coatings grown on the rough (average roughness $R_z \approx 1$ μm) beryllium and aluminum substrates (Fig. 3).

The [100] texture perfection degree measured by ψ-scanning [8] varied non-monotonically. For the coatings deposited at 600–700°C, a significant diffraction line narrowing was observed using ψ-scanning, which indicates the decrease of the crystallite angular disorientation with respect to the [100] texture axis (Fig. 4). An interesting feature was the increasing texture perfection as the coating thickness rised (in Fig. 4, the data for about 1 μm thick condensates are presented along with the 0.5 μm condensate for comparison). Moreover, it should be noted that for the condensates obtained at $T_{cond} > 830$°C (under sputtering the 3rd composition target) and at $T_{cond} > 900$°C (under sputtering the 2nd composition target) the single (W,Ti)C solid solution peak divided into two sub-peaks corresponding WC and TiC constituents, hence, the single-phase state was broken (Fig. 5). In Fig. 5, the typical (331) and (420) reflections of the solid solution are shown prior to and after the solid solution decomposition into WC and TiC. In this case, the solid solution condensates were obtained by sputtering the of the 2nd composition target (21 mol.% TiC, 79 mol.% WC).

The kinetics of the phase composition change depending on variation of the Ti/W atomic ratio in the target being sputtered and the substrate temperature in the range 80–900°C under condensation has shown (Fig. 6) that for the 1st target with relatively high titanium concentration, the condensates retained the single phase state up to the highest (950°C) deposition temperature studied (Fig. 6a). The sputtering of the targets with lower titanium content (targets 2 and 3) resulted in formation of a single-phase solid solution condensate at temperatures not exceeding 750°C (Fig.6, b, c). For the condensates sputtered from the 2nd target and deposited at higher temperatures of 800 to 850°C, the diffraction lines of both W_2C phase (with HCP lattice, Fig. 6b), and α–W are revealed. More pronounced (due to the higher volume content) is the formation of W_2C and α–W crystallites in the conden-

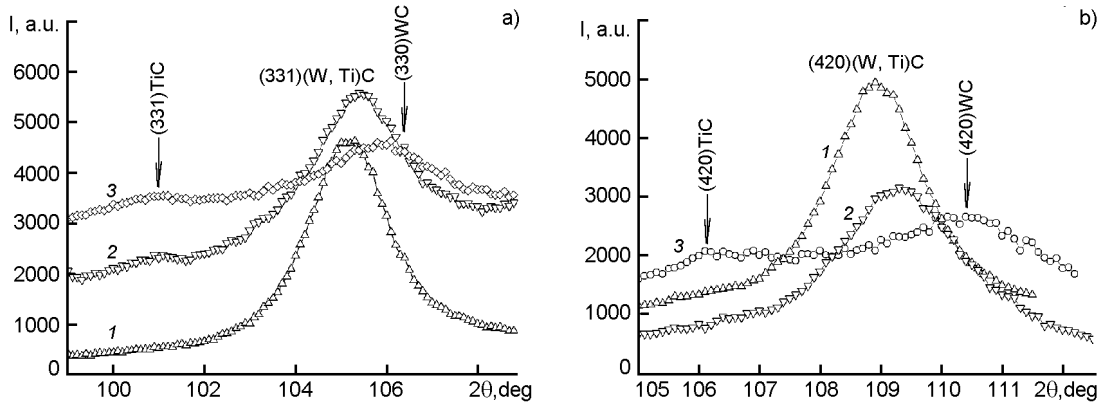

Fig. 5. Partial views of diffraction spectra for the condensates deposited by sputtering the 2nd composition target onto silicon substrates at different temperatures: 700 (*1*), 850 (*2*), 950°C (*3*).

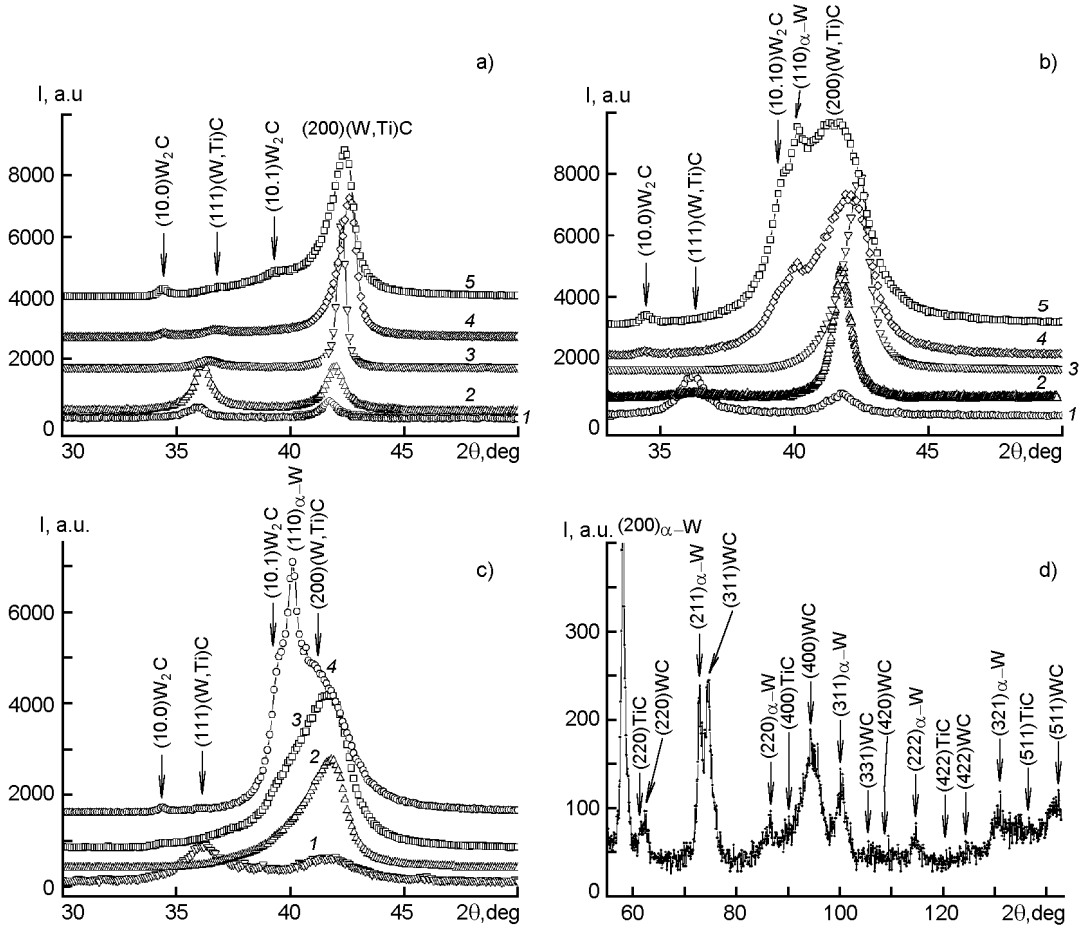

Fig. 6. Partial views of diffraction spectra for the condensates deposited by sputtering the targets of different compositions at different temperatures: (a) 31 mol.% TiC–69 mol.% WC (T_c = 250 (*1*), 560 (*2*), 850 (*3*), 900°C (*4*), 950°C (*5*)), (b) 21 mol.% TiC–79 mol.% WC (T_c = 80 (*1*), 300 (*2*), 700 (*3*), 850°C (*4*), 950°C (*5*)), (c) 15 mol.% TiC–85 mol.% WC (T_c = 80 (*1*), 700 (*2*), 750 (*3*), 850°C (*4*)), (d) 15 mol.% TiC–85 mol.% WC (T_c = 850°C).

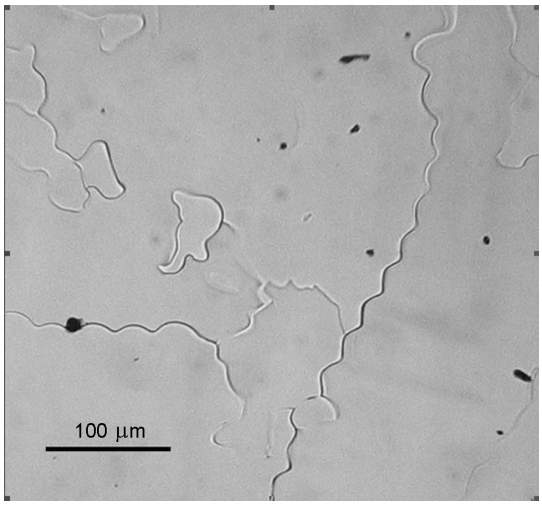

Fig. 7. A photo of the film surface after condensation at 80°C.

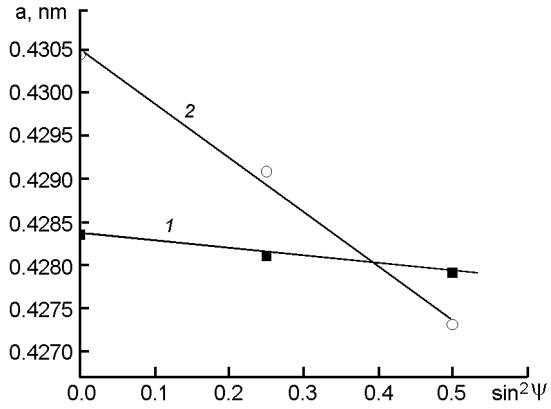

Fig. 8. a–$\sin^2\psi$ plot for macro-strain determination in the condensate of (W,Ti)C solid solution (the target composition 79 mol.% WC–21 mol.% TiC, T_c = 80°C, the substrates of beryllium (*1*) and silicon (*2*)).

sates sputtered from the 3rd target (with the lowest Ti content) and deposited at 850°C (Fig. 6, c–d). In this case, the predominant formation of α–W phase is revealed together with WC and TiC carbides as a result of the (W,Ti)C solid solution decomposition (Fig. 6d). Thus, during high temperature deposition from the target with low titanium content, three main phases are formed: titanium and tungsten mono-carbides, and α–W with the BCC lattice. Under equilibrium conditions, such a reaction of the lower tungsten carbide (W_2C) formation followed by its decomposition into the almost pure α–W and tungsten mono-carbide (WC) takes place under carbon deficiency at 1255°C [9], i.e. substantially above the substrate temperatures used.

It is known that the phases with lower carbon content as compared to the initial mono-carbide are formed by creation of an ordered vacancy sub-system in the carbon sub-lattice [15]. As it is seen from Fig. 4 and 6, that process is most intensive in the [100] textured condensates deposited onto a smooth surface, for example, the silicon, providing both sufficiently high mobility of deposited atoms and a rather small scattering angle after the collision of the atoms with the surface. Thus, both the planarity of the coating and the high mobility of carbon atoms under condensation above 700°C results in an intensive carbon re-evaporation followed by leaving the condensate deposition zone. This process is most pronounced in the tungsten enriched domains where the carbon depletion results in growth of the crystallites with a strong metallic binding stimulating the formation of BCC lattice typical for the pure tungsten. The decomposition of a carbon-deficient (Ti,W)C solid solution results in formation of titanium mono-carbide crystallites only, while both a lower tungsten carbide and the tungsten phase being formed besides of the tungsten mono-carbide crystallites. This indicates a higher strength of Ti–C bond as compared to W–C one. This suggestion agrees well with the Ti–W–C equilibrium diagram: the (Ti,W)C solid solution unsaturated in carbon decomposes just into two phases, W and (Ti,W)C, but not into two simple carbides [9]. Indeed, due to a high contribution of the metallic d(W–W) bond, the W–C binding is significantly weaker than the Ti–C one [15], that is the reason for the predominant decarburization and formation of domains enriched in tungsten. In this case, according to the reaction: $WC + O_2 \rightarrow W + CO_2$, the free energy gain is $\Delta H_{900K} = -435$ kJ/mol. [17]. The volatile CO_2 is removed from the condensation area due to the continuous evacuation.

Besides of the high atomic mobility stimulated by the vacancy sub-system in metallic and non-metallic sub-lattices, one of the main reasons for the formation of lower carbides and the (W,Ti)C solid solution decomposition into WC and TiC could be the condensation stress development [10]. Considering the effect of the condensation stresses, it should be noted that at low substrate temperature (80°C), the condensate is torn off immediately during deposition, the tearing boundary having a wave-like periodic appearance as shown in Fig. 7.

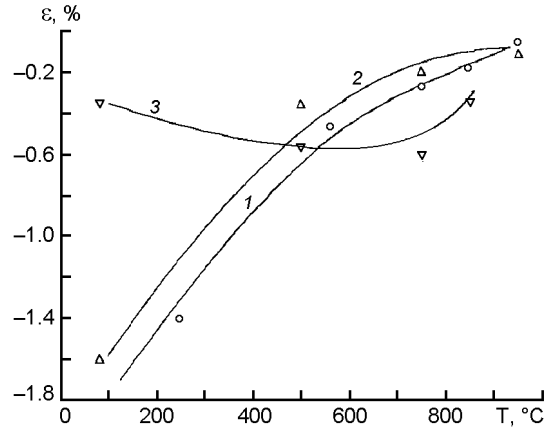

Fig. 9. Macro-strain values vs deposition temperatures onto silicon substrate for the condensates obtained by sputtering the targets of different compositions: 31 mol.% TiC–69 mol.% WC (*1*), 21 mol.% TiC–79 mol.% WC (*2*), 15 mol.% TiC–85 mol.%

The macro-strains measured by the method of multiple oblique scans were found to be compressive in the coatings deposited at 80°C onto silicon substrates with good adhesion; a rather high strain $\varepsilon \approx -1.6$ % determined from the a–$\sin^2\psi$ plot (Fig. 8) is close to the critical value for the ion-plasma carbide condensates [11]. For the coatings deposited at 80°C onto both beryllium and silicon substrates, the average composition was considered to be constant over the sample thickness and independent of the substrate type. Thus, the slopes of a–$\sin^2\psi$ plots were assumed to be defined only by the strain value and the point of intersection at $\sin^2\psi = 0.39$ was meant as corresponding to the unstrained section for the cubic lattice ($\sin^2\psi_0 = 2\mu(1 + \mu)$ [12]. So, the lattice parameter for the unstrained section is 0.42814 nm, and Poisson coefficient is estimated as $\mu \approx 0.24$.

A highly perfect texture ($\Delta\psi < 15°$) in the coatings deposited at temperatures above 600°C (Fig. 4) caused the necessity to measure (331), (420), (422), (511), and (333) reflections at corresponding crystallographic angles of 46.5, 26.5, 35.3, 15.7 and 54.7° with respect to the normal to (100) plane [5]. As it is known, the formation of packing defects is inherent in the tungsten carbide condensates prepared at high substrate temperatures [13], only the (333) and (422) reflections not shifted by packing defects and the (511) reflection with small effect thereof were used to plot the a–$\sin^2\psi$ relationship.

The resulting macro-strain values for different compositions and condensation temperatures are shown in Fig. 9. It is seen that at a high condensation temperature and a relatively high TiC content in the condensates, the high macro-strains develop

Table. Condensate composition calculation by the variation of lattice parameter in non-stressed state.

Sputtered target composition	Deposition temperature, °C	Si substrate				Be substrate			
		a_{in}, nm	a_{red}, nm	$a_{red}(T_c)/a_{red}(T_{80/250C})$	X^{**}	a_{in}, nm	a_{red}, nm	$a_{red}(T_к)/a_{red}(T_{80/250C})$	X^{**}
31 mol.% TiC–69 mol.% WC	250	0.42972	0.42972	–	–	–	–	–	–
	560	0.4292	0.4293	≈1	1	–	–	–	–
	760	0.42844	0.42869	0.9989	0.95	–	–	–	–
	850	0.42702	0.42742	0.9947	0.79	–	–	–	–
21 mol.% TiC–79 mol.% WC	80	0.42814	0.42814	–	–	0.42814	0.42814	–	–
	560	0.4272	0.4273	0.9980	0.90	0.4275	0.4276	0.9987	0.94
	700	0.42523	0.42573	0.9944	0.78	0.42538	0.42588	0.9947	0.79
	850	0.42384	0.42451	0.9915	0.73	0.42447	0.42516	0.9930	0.755
15 mol.% TiC–85 mol.% WC	80	0.42774	0.42774	–	–	0.42775	0.42775	–	–
	500	0.42675	0.42689	0.9980	0.90	0.42685	0.42699	0.9982	0.92
	700	0.42501	0.42530	0.9943	0.77	0.42519	0.42537	0.9944	0.78
	850	0.42303*	0.42405	0.9913	0.725	0.42405	0.42437	0.9921	0.745

* — determined for WC phase at the full phase separation of (W,Ti)C-solid solution into WC and TiC constituents.

** — the value of x in the formula $(W,Ti)C_x$ is given from [15].

and remain non-relaxed. Those compressive macro-strains reach a value of −1.6 % which is close to the critical value for carbide condensates [11, 14]. However, at a high condensation temperature but at a low TiC content, the macro-strains being relatively low, not exceeding −0.3 %. The non-linear behavior in the 750–900°C range is assumed to be due to the multiphase material formation (Fig. 6, b, c, d). At the same time, in the (W,Ti)C solid solution condensates deposited onto the polished nickel substrates with high thermal expansion coefficient ($\alpha_{Ni} \approx 17.1 \cdot 10^{-6}$ deg^{-1}), a large value of condensation compressive strain (−1.05 to −1.4 %) was retained in the coating even at the high deposition temperature 850–900°C (under sputtering the targets of the 1st and 2nd contents).

The main factors affecting the ion-plasma condensate final structure state are known to be the difference of thermal expansion coefficients for the condensate, λ_c, and the substrate, λ_s, ($\Delta\lambda = \lambda_c - \lambda_s$), and the "atomic peening" condensation strains due to deposited particle bombardment of the growing coating [12]. Assuming the "atomic peening" strains to depend slightly on the substrate type at a relatively large condensate thickness, the observed differences between the condensates deposited onto Si and Ni substrates may be explained by the $\Delta\lambda$ difference. The evaluations show that the macro-strain values obtained might be the case at $\lambda_{Si} << \lambda_c \approx \lambda_{Ni}$. It is to note that the compressive macro-strain values in the condensates deposited onto the rough aluminum and beryllium substrates were lower, not exceeding −0.25 %.

Taking into account the macro-strain effect, it is possible to determine the lattice parameter in the "non-stressed" section from the a–$\sin^2\psi$ plot. This parameter is related only with structure state of the lattice itself. The values of the "non-stressed" lattice parameters are presented in Table for all the compositions and deposition temperatures used. In the Table, the reduced parameter values are given, which include the elemental composition variations in the metallic sub-lattice (Ti/W ratio in Fig. 1) at higher deposition temperature compared to the lowest one (80–250°C). The reduced parameter (a_{red}) was calculated according to Vegard's rule for substitution solutions from the experimental value ain using the equation $a_{red} = a_{in} + \Delta C_{Ti} \cdot K$. Here ΔC_{Ti} is the difference between titanium atomic concentrations in the condensates deposited at low (80–250°C) and high (above 500°C) substrate temperatures. The K value is determined by the lattice parameter increase due to substitution of 1 % W atoms by Ti atoms in the carbide, and estimated to be $6.3 \cdot 10^{-5}$ nm ($a_{TiC} = 0.4330$ nm, $a_{\beta\text{-}WC} = 0.4267$ nm [15]). Thus, comparing the values of the reduced parameters for the coatings deposited at high condensation temperature ($a_{red}(T_c)$) with the "low temperature" parameter ($a_{red}(T_{80/250C})$) and using the data from [15], we could estimate the variation of the carbon atomic concentration in the carbide.

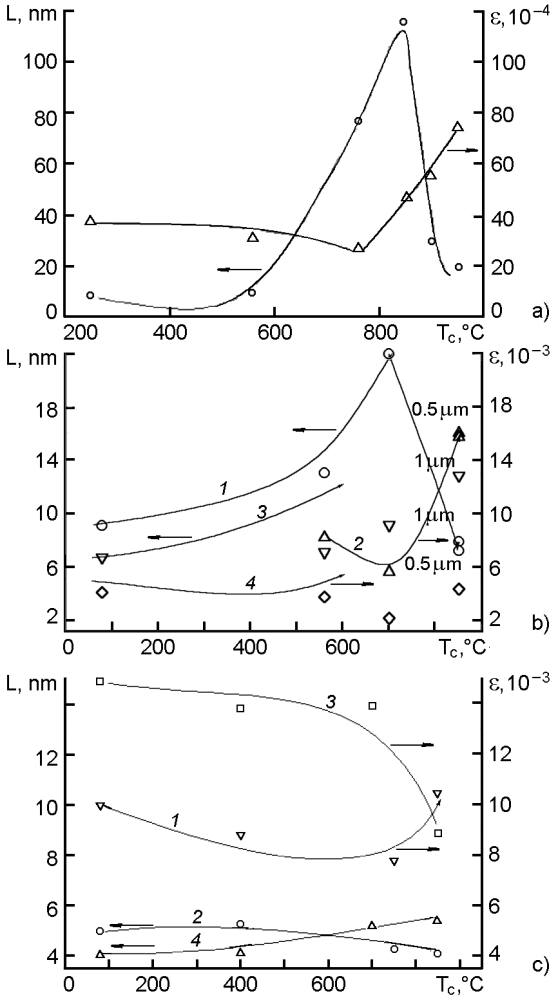

Fig. 10. Effect of the substrate temperature on the sub-structure features of nano-crystalline WC–TiC system condensates obtained by sputtering the targets of different compositions: (a) 31 mol.% TiC–69 mol.% WC (silicon substrate), (b) 21 mol.% TiC–79 mol.% WC (silicon (*1*, *2*) and beryllium (*3*, *4*) substrates), c — 15 mol.% TiC–85 mol.% WC (silicon (*1*, *2*) and beryllium (*3*, *4*) substrates).

As it is seen from Table, at the condensation temperatures lower than 500–560°C, the composition remains close to stoichiometric one in carbon atoms, i.e. $x \approx 1$. At 700°C deposition temperature, and particularly at temperatures of 800–850°C, a significant x decrease down to the critical value of 0.74 is observed. This value is the critical because at lower x values, decomposition of the solid solution followed by formation of a multiphase condensate takes place.

In general, it could be noted that the condensation temperature rise results in decreasing lattice parameter. Such the lattice parameter variation is related with increasing specific contribution from the metallic bond as the condensation temperature increases as well as with high concentration of non-equilibrium vacancies formed in the carbon sublattice.

The average crystallite sizes and micro-strains were calculated by usual technique [16] using two reflection orders. In Fig. 10, the plots are shown for the condensates deposited from three types of the targets. It should be noted that the substructure characteristics of the condensates deposited onto beryllium substrates in the whole temperature range correspond to (W,Ti)C solid solution nano-crystallites, while at a relatively low Ti atomic concentration and deposition temperature 850°C on the silicon substrate, the solid solution decomposes, and besides of the (W,Ti)C solid solution crystallites (or of WC and TiC formed due to (W,Ti)C solid solution decomposition), the crystallites of a lower tungsten based carbide phase (W_2C) or the crystallites with a BCC lattice inherent in α–W phase are formed (Fig. 6).

As it is seen from Fig. 10, at relatively low deposition temperatures, a characteristic variation of substructure features in the single-phase condensates is observed: the coherence length increases and the micro-strains decrease as the deposition temperature rises. However, in the temperature range from 700 to 900°C, where the processes of the second phase pre-precipitation and precipitation are possible, a reverse behavior is observed. In this area, at first the micro-strain increase in the solid solution crystallites occurs, while the crystallite average size decreasing. At high titanium atomic concentration (1st series) as well as at condensation onto the rough beryllium substrate, the crystallite sizes increase up to the highest condensation temperature, while the crystallite micro-strains either decrease monotonically or slightly increase in the temperature range of 700 to 850°C (Fig. 10).

A diminution of the average crystallite size and increase of micro-strain value in the (W,Ti)C solid solution phase or in the β–WC constituent could be connected with formation of a multi-phase material on the silicon substrate at high deposition temperature (850°C). For the condensate with the lowest titanium content (obtained from the 3rd target sputtering), the second major phase was α–W phase besides of the (W,Ti)C solid solution (Fig. 6c,d). The α–W crystallites showed a relatively low micro-strain level (0.08 %), and the α–W crystallite average size (about 6 nm) was smaller compared to the solid solution (W,Ti)C crystallites. As the condensate thickness grew, the (W,Ti)C solid solution crystallite average size increased and the micro-strains decreased (see, for example, Fig. 10b).

The analysis of the condensate structure state indicates that after the solid solution decomposition, the predominant orientation remains in the carbide phase crystallites, while the α–W metallic phase crystallites formed due to carbon escape are non-oriented. A typical diffraction spectrum measured using Bragg-Brentano focusing is presented in Fig. 6d. In this connection, the carbon atomic diffusion under the high-temperature crystallite formation could result in the metallic binding strengthening and disorients the α–W crystallites. Thus, the absence of α–W crystallite predominant orientation along with remaining both the (W,Ti)C solid solution and WC and TiC textures indicates the important role of Me–C binding for the formation of highly oriented crystallites in ion-plasma condensates of the quasi-binary carbide system.

To conclude, in the condensates deposited using the ion-sputtering of the quasi-binary WC–TiC targets, the formation of the single-phase (W,Ti)C solid solution with the cubic lattice inherent in TiC phase takes place within a wide concentration range. At the relatively low condensation temperature (<300°C) no significant structure differences have been observed independently of the substrate type and roughness level thereof. The characteristic predominant [100] orientation has been revealed in the condensates deposited onto the smoothly finished silicon substrate (as well as onto glass ceramic and nickel substrates) at the condensation temperatures exceeding 300°C.

Under the high temperature ion-plasma deposition, the multiphase formation of the quasi-binary WC–TiC carbide on a silicon substrate smooth enough correlates with the [100] growth texture development in the solid solution crystallites, which manifests itself most at the condensation temperature 700°C. The textures with [100] axis perpendicular to the growth plane results in appearance of easy diffusion ways, followed both by changing the diffusion processes kinetics and the steep lattice parameter decrease (Table).

At atomic ratios Ti/W≤0.25 and condensation temperatures exceeding 850°C on the finished substrate, four phases are formed instead of a single-phase (W,Ti)C solid solution: β–WC (NaCl type lattice); TiC (NaCl type lattice); α–W (BCC lattice) and traces of W_2C (hexagonal lattice). Under deposition onto rough beryllium (as well as onto aluminum to T_c≤600 °C) substrate, neither the crystallite predominant orientation in the whole temperature range, nor the solid solution decomposition into lower carbides at 850°C deposition temperature was observed. The (W,Ti)C solid solution formed on the nickel substrates remains practically stable.

Application of the X-ray multiple oblique scans for macro-strain measurements has revealed a regularity characteristic for the condensates: the (W,Ti)C solid solution stable state up to high temperatures are observed in the condensates subjected to high compressive strains. This is the case both for the condensates deposited at low temperatures (300°C and lower) onto all the substrate types, and for those deposited at high temperature onto smooth substrates with a high thermal expansion coefficient.

Acknowledgment. The author thanks the leading researcher Ph.Dr.A.N.Stetsenko for preparation of the ion-plasma condensates.

References

1. O.V.Sobol', *Functional Materials*, **13**, 387 (2006).
2. O.V.Sobol', O.N.Grigorjev, Yu.A.Kunitsky et al., *Science of Sintering*, **38**, 63 (2006).
3. O.V.Sobol', *Functional Materials*, **13**, 577 (2006).
4. O.V.Sobol', *Phys. Solid State*, **49**, 1161 (2007).
5. O.V.Sobol', E.A.Sobol, A.A.Podteleznikov, *Functional Materials*, **6**, 868 (1999).
6. S.H.Koutzaki, J.E.Krzanowski, J.J.Nainaparampil, *Metallurg. and Mater. Transact. A*, **33**, 1579 (2002).
7. O.V.Sobol', in: Proc. of 5th Int. Conf. on Equipment and Technologies for Thermal Treatment of Metals and Alloys, Vol.2, NNTs KhPhTI, IPTs "Kontrast", Kharkiv (2004), p.241.
8. O.V.Sobol', *Nanosystems, Nanomaterials, Nanotechnologies*, **4**, 707 (2006).
9. T.B.Gorbacheva, X-ray Investigations of Hard Alloys, Metallurgia, Moscow (1985) [in Russian].
10. A.P. Shpak, O.V.Sobol', P.G.Cheremskoy et al., *Nanosystems, Nanomaterials, Nanotechnologies*, **4**, 412 (2006).
11. O.V.Sobol', in: Proc. of 7th Int. Conf. on Equipment and Technologies for Thermal Treatment of Metals and Alloys, Vol.3, NNTs KhPhTI, IPTs "Kontrast", Kharkov (2006), p.72.
12. O.V.Sobol', *Fiz. Metal. i Metalloved.*, **91**, 63 (2001).
13. O.V.Sobol', E.A.Sobol', L.I.Gladkikh, A.N.Gladkikh, *Functional Materials*, **9**, 486 (2002).
14. A.A.Koz'ma, O.V.Sobol', E.A.Sobol' et al., *Functional Materials*, **6**, 267 (1999).
15. G.V.Samsonov, G.Sh.Upadkhaya, V.S.Neshpor, Physical Materials Science of Carbides, Naukova Dumka, Kiev (1974) [in Russian].
16. S.S.Gorelik, Yu.A.Skakov, L.N.Rastorguyev, X-ray and Electron-Optic Analysis, MISIS, Moscow (1994) [in Russian].
17. A.A.Koz'ma, O.V.Sobol', E.A.Sobol', *Vestnik KhGU, Ser. "Fizika"*, **440**, 149 (1999).

Вплив термічного фактора на процес фазоутворення, структуру, субструктурні характеристики та напружений стан нанокристалічних іонно-плазмових конденсатів квазібінарної системи WC–TiC

О.В.Соболь

Методами ширококутової рентгенівської дифрактометрії та рентгенофлуоресцентного спектрального аналізу вивчено вплив складу матеріалу, що розпилюється, та температури осадження на фазовий та елементний склад, структуру, субструктурні характеристики та напружений стан іонно-плазмових конденсатів квазібінарної системи WC–TiC. Встановлено, що збільшення відносного атомного вмісту титану в конденсаті призводить до підвищення верхньої межі температурної стабільності однофазного ((W,Ti)C-твердий розчин) стану при атомному співвідношенні Ti/W≥0.35 до 950°C. При атомному співвідношенні атомів Ti/W≤0,25 і температурі осадження вище 800°C утворюється багатофазовий конденсат, який складається з нижчого карбіду W_2C, практично чистого α–W з ОЦК решіткою, WC та TiC фаз, які утворюються внаслідок розпаду (W,Ti)C-твердого розчину. При формуванні однофазного твердого розчину розмір кристалітів з підвищенням температури конденсації збільшується, а величина мікродеформації — зменшується. При формуванні багатофазових покриттів середній розмір кристалітів зменшується, а рівень мікродеформації збільшується. Проведено оцінку вмісту вуглецю у (W,Ti)C-твердому розчині, та встановлено критичну температуру осадження 700°C, вище за яку інтенсивно утворюються вакансії у вуглецевій підгратці карбіду. Обговорюються фізичні причини ефектів, що спостерігаються, і виявлених закономірностей.